Changes in estuarine sediment phosphorus fractions during a large-scale Mississippi River diversion

Eric D. Roy[1][*], Nhan T. Nguyen[2], and John R. White[2]

[1]Rubenstein School of Environment and Natural Resources, University of Vermont, Burlington, VT 05405, United States
[2]Department of Oceanography and Coastal Sciences, College of the Coast and Environment, Louisiana State University, Baton Rouge, LA 70803, United States

*Corresponding author: eroy4@uvm.edu

Abstract

Ongoing deterioration and loss of wetlands in the Mississippi River delta threatens the survival of Louisiana's coastal ecosystems and human settlements. In response, the state of Louisiana has initiated a $50 billion, 50-year restoration program. A central piece of this program is the reintroduction of Mississippi River water into the deltaic plain using managed diversions that mimic natural flood pulses. These diversions would transport critically needed sediment, but also deliver large nutrient loads. Coastal eutrophication is therefore a concern, particularly blooms of toxin-producing cyanobacteria. The Bonnet Carré Spillway (BCS) is an existing large flood diversion that protects New Orleans and provides an opportunity to investigate diversion nutrient transport. Here, we quantify sediment phosphorus (P) deposited by the BCS for the first time, and use a sequential P fractionation scheme to evaluate the likelihood of future sediment P release to the water column of the Lake Pontchartrain Estuary. In 2011, we collected sediment cores in the estuary for determination of P fractions before and after the discharge of 21.9 km^3 of river water through the BCS in just under 6 weeks. We observed the greatest net increases in sediment total P, inorganic P forms, and less recalcitrant organic P in the region near the inflow. We estimate that the diversion deposited $\geq$ 5,000 metric tons of P in the sediments of the Lake Pontchartrain Estuary. Approximately 20-30% of post-diversion sediment P existed as readily available inorganic P, Fe/Al-bound P, or more labile organic P, forms which are more likely to contribute to internal P loading to the water column. Diversion designs that encourage sedimentation in coastal marshes versus open bays can likely reduce the chances that deposited particulate P creates eutrophication risk.

66

67

68

69

70

71

72

73

74

75

76

77

78

79

80

81

82

83

84

85

86

1. Introduction

The flood pulse is a principle driving force influencing sediment transport, nutrient availability, and the productivity of biota in river-floodplain systems and estuaries (Junk et al. 1989, Day et al. 1995). Widespread human modification of hydrology in coastal zones has reduced the influence of freshwater pulsing events in many estuaries (Giosan et al. 2014). Today, efforts are underway to restore freshwater pulses in degraded coastal ecosystems, including the Mississippi River delta (State of Louisiana 2017). The reintroduction of Mississippi River water into the deltaic floodplain using managed diversions that mimic natural functioning offers several ecosystem benefits, including sediment provision (Day et al. 2016). However, potential unintended consequences of freshwater pulses into Louisiana's estuarine environments remain a concern, including the perceived threat of nutrient-fueled blooms of toxin-producing cyanobacteria (Turner et al. 2004, Ren et al. 2009). Due to the human-induced nutrient enrichment of the Mississippi River, like many other large rivers, restoring hydraulic connectivity can dramatically affect nutrient delivery to receiving estuaries (Roy et al. 2013). Clarifying both the direct and indirect biogeochemical pathways by which these nutrients can drive estuarine toxic cyanobacteria bloom formation is imperative given the economic and cultural importance of Louisiana's coastal fisheries.

The Bonnet Carré Spillway (BCS) is a flood control structure used by the US Army Corps of Engineers to protect the city of New Orleans, LA from Mississippi River flooding (Fig. 1). This structure diverts Mississippi River water (up to 17% of the design flood stage) into the Lake Pontchartrain Estuary (LPE), with variability in diversion timing and discharge (Roy et al. 2013). Recent BCS openings have occurred in 1997, 2008, 2011, and 2016. These events provide

109   an opportunity to study sediment transport, clarify diversion-bloom links, and inform coastal

110   restoration efforts (Nittrouer et al. 2012, Roy et al. 2013). In 2011, the US Army Corps opened

111   the BCS between May 9 and June 20, discharging 21.9 km^3 of freshwater (330% of the estuary's

112   typical volume) and immense nutrient loads, influencing most of the LPE (Roy et al. 2013). The

113   upper 10-15% layer of river water was diverted through the BCS carrying suspended sediment,

114   including mud (silt and clay) and 31-46% of the river's sand load (Nittrouer et al. 2012). Local

115   river conditions resulted in the diversion of sandy bed sediment, much of which was deposited in

116   the first 2.5 km of the BCS. Lighter mud remained in suspension to the LPE due to bed stress

117   (Nittrouer et al. 2012). The river plume deposited an estimated 2.45±1.35 MT of sediment in the

118   LPE (Fabre 2012).

119   The Mississippi River carries multiple forms of P. Approximately 40-50% of the total P

120   carried in the surface waters of the Mississippi River entering the BCS in 2011 was soluble

121   reactive P (SRP), with the remainder in particulate forms (Mize et al. 2012). Such measurements

122   are not necessarily representative of the river water column, including P bound to heavier

123   sediments in deeper portions (Mayer et al. 1998, Sutula et al. 2004). Previous researchers have

124   found that iron-bound P represented to largest fraction of P in Mississippi River suspended solids

125   (Sutula et al. 2004). This Fe-P is largely redox sensitive and can be released under anaerobic

126   conditions typical of estuarine sediments (Zhang et al. 2012). Past work suggests that all SRP

127   loaded by the BCS during the 2011 event was removed from the water column within the LPE,

128   primarily due to assimilation by phytoplankton, which was followed by an SRP rebound post-

129   diversion driven by internal loading (Roy et al. 2013, Fig. 2). However, the fate of particulate P

130 carried by the diverted river water has not been examined, and was the motivation of the present

131 study.

132   Past BCS research has revealed that direct cyanobacteria bloom stimulation by nutrient-

133 rich river water does not always occur during BCS openings and likely depends on diversion

134 timing (Turner et al. 2004, Mize and Demcheck 2008, White et al. 2009, Bargu et al. 2011, Roy

135 et al. 2016). Instead, chlorophytes and/or diatoms outcompete cyanobacteria in turbulent, light-

136 limited, and nutrient-rich diverted Mississippi River water (Roy et al. 2016). However, blooms

137 of cyanobacteria, including nitrogen fixers *Anabaena* spp. and *Cylindrospermopsis raciborskii*,

138 have been observed in the weeks and months after BCS closure on occasion (e.g., 1997, 2008),

139 the exact mechanisms of which remain unclear (Turner et al. 2004, Mize and Demcheck 2008,

140 Bargu et al. 2011). We suspect that internal loading of P from sediments is one important

141 mechanism (Roy et al. 2012), and that diversions may increase the sediment P stocks that

142 contribute to it.

143   In this study, we quantified sediment phosphorus (P) deposited by the BCS in 2011, and

144 used a sequential P fractionation scheme to evaluate the likelihood of sediment P release to the

145 water column of the Lake Pontchartrain Estuary over time. Additionally, we monitored water

146 column suspended solids across a transect extending from the BCS inflow toward the center of

147 the LPE during the diversion. We hypothesized that surface sediment total P concentrations

148 would increase following the diversion, especially in the region near the BCS inflow where

149 heavier mineral solids would settle out of the freshwater plume as velocity decreased.

150 Furthermore, we hypothesized that less stable sediment P forms (i.e., readily available inorganic

151 P, redox-sensitive Fe-bound inorganic P, and labile organic P) would increase following the

152 diversion, indicating increased availability of P for release to the water column.

153 **2. Methods**

154 *2.1. Study site*

155   The LPE is a wind-driven estuary in southeast Louisiana, USA that is shallow (mean

156 depth = 3.7 m, with minor short-term increase during diversions depending on wind direction)

157 and oligohaline (salinity = 2-9; Li et al. 2008) (Fig. 1). The 1637 km^2 estuary receives freshwater

158 input from the fresher Lake Maurepas, several northern tributaries, and urban New Orleans

159 (Turner et al. 2002). Water exiting eastern Lake Pontchartrain eventually enters the Gulf of

160 Mexico following passage through Lake Borgne. Most of the shallow sediments in the LPE

161 derive from erosion of the Pleistocene terraces to the north and the Holocene delta plain to the

162 south, and sedimentation is now restricted because bed load influx from the Mississippi and

163 Pearl Rivers has been minimal since the Holocene (Flocks et al. 2009). Sediments to 3 m depth

164 are generally massive muds, with bioturbation and shells throughout (Flocks et al. 2009). Surface

165 (top 10-12 cm) sediment measurements taken in 2003 (147 samples collected on an ~8 km grid

166 across entire LPE) indicated a lake-wide mean (±1 std. dev.) total P content of 403±199 mg P kg^{-1}

167 ^{1} dry sediment (DeLaune et al. 2008). Historical data concerning the eutrophication status of the

168 system are so scarce that it is not possible to evaluate temporal trends (see Roy et al. 2013 and

169 2016 for discussion and citations).

170 *2.2. Water column suspended solids*

171   Surface water samples (depth = 10 cm) were collected along a 10-station, 30-km transect

172 extending northeastwardly from the BCS inflow to the Lake Pontchartrain Causeway (Fig. 1) on

173 four dates in 2011 when the BCS was open (May 18, May 28, June 4, June 16) and two dates

174 immediately following BCS closure (June 21 and 25). Total suspended solids (TSS) were

175 quantified by filtering a measured volume of water through a pre-ashed glass fiber filter (GFF

176 Gelman), followed by drying at 105°C, and weighing. Filters were burned at 550°C to determine

177 the total volatile solids (TVS) content as loss on ignition. Inorganic suspended solids were then

178 calculated as the difference between TSS and TVS.

179 *2.3. Sediment sampling and characterization*

180   Sediment cores were collected from 15 stations in the LPE using a piston corer on May 8,

181 2011 (one day before BCS opening) and again on July 7, 2011 (17 days after BCS closure).

182 Cores (one per station) were sectioned into 0-5 cm and 5-10 cm intervals immediately after

183 return from the field for sediment characterization. The 10-cm layer likely takes a decade or

184 longer to be deposited under normal conditions (Flocks et al. 2009). However, following BCS

185 diversions, visual inspections of cores has revealed 10 cm or more of new sediment in some

186 "near" stations, indicated by a layer of reddish, oxidized sediment immediately after closure.

187   Sediment analyses included moisture content (gravimetric method including drying at 70º

188 C), bulk density, loss on ignition (550°C muffle furnace for 4 h), total carbon (TC) and nitrogen

189 (TN) (Elemental Combustion System with a detection limit of 0.005 g kg^{-1}, Costech Analytical

190 Technologies. Inc., Valencia, CA), and total metals (Al, Fe, Ca, Mg). Total metals were

191 determined following the method described by Malecki-Brown and White (2009). Briefly, a

192 dried ground sample (~0.5 g) was placed in a 50-mL beaker at 550˚C for 4 h. Next, 20 mL of 6

193 *M* HCl was added into the beaker, which was then placed on a 120˚C hot plate for 5 h to dissolve

194 all metals. The digested sample was filtered (Whatman #42) and diluted in a 50-mL volumetric

195 flask using deionized water. Finally, the filtrate was analyzed on a Varian model inductively

196 coupled plasma elemental analyzer (MPX ICP-OES). Sediment characteristics (aside from

197 moisture) are reported on a dry weight basis.

198 *2.4. Sediment phosphorus analysis*

199   For total P (TP), dried ground sediment samples (~0.3 g) were added into 50-mL glass

200 beakers, which were then placed into a 550°C muffle furnace for 4 h to burn off all organic

201 content. After cooling, 20 mL of 6 M HCl was added and samples were heated on a hot plate at

202 130°C for 5 h, dissolving all inorganic P forms contained within minerals remaining in the

203 sediment sample (Anderson 1976). The solution was then filtered (Whatman #42) and diluted in

204 a 50-mL volumetric flask. The filtered sample was analyzed for TP on a Seal Analytical AQ2

205 discrete colorimetric analyzer (Method 365.1; USEPA 1993).

206   A sequential P fractionation method was used on field moist sediment samples (1-2 g)

207 that operationally separates five different pools of P in sediments: (1) readily available inorganic

208 P_i [*20 mL 1 M KCl extraction for 1 h*], (2) Fe/Al-bound P_i [*20 mL 0.1 M NaOH extraction for 17*

209 *h*], (3) alkali extractable organic P_o [*= NaOH-TP - NaOH-P_i*], (4) Ca/Mg-bound P_i [*20 mL 0.5 M*

210 *HCl extraction for 24 h*], and (5) residual P [*residual TP digestion using method described*

211 *above*] (Reddy et al. 1998, White et al. 2004, Richardson and Reddy 2013, Adhikari et al. 2015).

212 After each extraction step, supernatants were immediately filtered (0.45 µm membrane filters),

213 filtrates were analyzed for soluble reactive P (SRP) (Method 365.1; USEPA 1993), and the

214 residual sediment was passed to the next extraction step. Centrifuge tubes were weighed after

215 each extraction step to correct for extracted P still present in the sample.

216   The NaOH extraction removes both Fe/Al-P_i and P associated with humic and fulvic

217   acids (Reddy et al. 1998). Therefore, after a subsample of the filtrate was first analyzed for SRP

218   to obtain Fe/Al-P_i (NaOH-P_i), a subsample was digested for TP analysis (NaOH-TP) to estimate

219   alkali extractable organic P_o (NaOH-P_o = NaOH-TP - NaOH-P_i). For the NaOH-TP digestion, 5

220   mL of the aliquot, 1 mL of 11 M H_2SO_4, and 0.35 g of $K_2S_2O_8$ were added to a digestion tube

221   and heated for 4 h at 150°C to remove water from the sample. The temperature was then

222   increased to 380°C for 4 h for complete digestion. After the completion of digestion, samples

223   were cooled, diluted with 10 mL deionized water before filtering (0.45 µm membrane filters),

224   and then filtrates were analyzed for SRP (Method 365.1, USEPA 1993). This method potentially

225   underestimates Fe/Al-P_i because the Fe extracted in this step can re-precipitate and potentially

226   remove phosphate from solution (DeGroot and Golterman 1990, Golterman 1996). Therefore,

227   the concentrations of Fe/Al-P_i extracted using this technique can be considered as a lower limit.

228   The residual P fraction can include refractory organic P and stable inorganic P forms (Reddy et

229   al. 1998, White et al. 2004). The sum of all P fractions (= readily available P_i + Fe/Al-bound P_i +

230   alkali extractable P_o + Ca/Mg-bound P_i + residual P) was compared with the direct TP

231   measurements to estimate the extraction efficiency of the fractionation scheme. Sediment P

232   characteristics are reported on a dry weight basis. A QA/QC procedure was used for all sediment

233   P analysis that tolerates 10% error.

234   The mass of different P fractions in each 5-cm sediment interval was calculated using the

235   following equation:

236    $$P_{mass} = P_{conc} \times BD \times h \times 10^{-2} \qquad\qquad [1]$$

237 where, P_{mass} = mass of P fraction in sediment interval (g P m^{-2}), P_{conc} = concentration of P

238 fraction in sediment interval (mg P kg^{-1} dry sediment), BD = bulk density (g dry sediment cm^{-3}),

239 and h = height of sediment interval (cm). P_{mass} values for the 0-5 cm and 5-10 cm intervals were

240 then summed for each sediment core, allowing calculation of the net change in P forms for the 0-

241 10 cm sediment layer between the pre-diversion and post-diversion samples for each location.

242 *2.5. Assessment of spatial trends*

243 Pre- and post-diversion individual sediment P pools, as well as other sediment

244 characteristics, were compared using nonparametric Wilcoxon signed rank tests. For all

245 comparisons, the stations were divided into two groups: "near" (1-17 km from BCS inflow) and

246 "far" (21-34 km from BCS inflow). Additionally, the relationship between the net change in

247 P_{mass} within the 0-10 cm sediment layer for different P forms and distance from the BCS was

248 investigated using simple linear regression. The resulting total P regression model was applied in

249 GIS to estimate P deposition in the LPE for the distance range covered by our sampling (up to 35

250 km from BCS inflow; grid size = 10 m x 10 m; Euclidean distance function used to assign

251 distance values to each cell). A more conservative estimate of the total P deposition in sediments

252 based on a quadratic model corresponding to the lower 95% confidence interval of the total P

253 versus distance regression is also reported. All statistics were performed in R (R Core Team

254 2015) and all geoprocessing in ArcMap 10.4.1 (ESRI).

255 **3. Results**

256 *3.1. Water column suspended solids*

257 During the BCS opening, TSS concentrations in the LPE reached as high as 124 mg L^{-1}

258 (May 18, 0.9 km from spillway inflow; Fig. 3). For this sample, inorganic suspended solids

259   accounted for 116 mg L^{-1}, with 8 mg L^{-1} being organic material. Inorganic suspended solids

260   concentrations at the site nearest the BCS inflow declined with time during the BCS opening as

261   discharge through the spillway decreased (Fig. 3). Decreases in surface water inorganic

262   suspended solids with distance from the BCS were apparent between May 18 and June 16. Most

263   inorganic solids had settled out of surface waters by approximately 12 km from the BCS during

264   this period (Fig. 4a). By June 25 (four days after BCS closure), inorganic solids concentrations

265   were < 7 mg L^{-1} across the entire transect (Fig. 4a) and did not increase above 10 mg L^{-1} through

266   the end of July. Organic suspended solids concentrations were variable over space and time

267   during May, June, and early July, ranging from below detection to 16 mg L^{-1} (Fig. 4b).

268   *3.2. Sediment characteristics*

269   "Near" sediments (n = 8, 1-17 km from BCS inflow) tended to have greater bulk density

270   and Ca, and lower moisture content, organic content (LOI), TN, Al, Fe, and Mg than "far"

271   sediments (n = 7, 21-34 km from BCS inflow) (Table 1). Few changes in non-P sediment

272   characteristics were detected between pre- and post-diversion sediments. Changes in pre- and

273   post-diversion Ca contents at "far" sites observed for both sediment intervals were not

274   statistically significant (p = 0.375 to 0.938). However, the post-diversion average Ca for the 0-5

275   cm interval equaled 57% of pre-diversion average Ca, while the post-diversion average Ca for

276   the 5-10 cm interval equaled 73% of pre-diversion average Ca. TN was significantly different in

277   the 0-5 cm sediment interval at "far" sites, with greater values post-diversion (p < 0.05; Table 1).

278   *3.3. Sediment phosphorus*

279   The sum of all P fractions (= readily available P_i + Fe/Al-bound P_i + alkali extractable P_o

280   + Ca/Mg-bound P_i + residual P) equaled 103±8% of the direct TP measurement on average (± 1

281 standard deviation), indicating excellent extraction efficiency ($n = 60$). "Near" sediments were

282 characterized by similar levels of total P and readily available P_i compared to "far" sediments,

283 both pre- and post-diversion. However, there were significant differences in other P fractions for

284 "near" versus "far" comparisons, including greater 0-5 cm NaOH-P_o at "far" sites pre-diversion,

285 lower Ca/Mg-P_i at "far" sites post-diversion for both sediment intervals, and greater residual P at

286 "far" sites post-diversion for both sediment intervals (Table 1).

287 Significant ($p < 0.05$) differences pre- and post-diversion in total P, readily available P_i,

288 Fe/Al-P_i, and residual P were found, with greater values for post-diversion samples in the 0-5 cm

289 sediment interval for "near" sites (Table 1, Fig. 5a). NaOH-P_o was less significantly different for

290 these samples ($p < 0.10$). For the 5-10 cm "near" samples pre- and post-diversion, total P, readily

291 available P_i, Ca/Mg-P_i, and residual P were all significantly different, with greater values post-

292 diversion ($p < 0.05$; Table 1, Fig. 5a). On average, relatively more labile and redox-sensitive P

293 forms (readily available P_i + Fe/Al-P_i + NaOH-P_o) comprised approximately 30% of total P in

294 both sediment intervals for the "near" samples post-diversion (Fig. 5a). The post-diversion

295 difference in total P was less pronounced, but still significant ($p < 0.05$), for both sediment

296 intervals at the "far" sites, driven by increases in residual P (Table 1, Fig. 5b). In the 0-5 cm

297 interval for "far" samples pre- and post-diversion, NaOH-P_o was significantly different with a

298 smaller values post-diversion, while Ca/Mg-P_i was significantly different post-diversion at "far"

299 sites for both 0-5 cm and 5-10 cm sediment intervals, with smaller values in both cases (Table 1,

300 Fig. 5b).

301 Net change in total P for the 0-10 cm sediment layer ranged from -2 to +24 g P m^{-2} and

302 was significantly negatively correlated with distance from BCS inflow ($r^2 = 0.35$, $p < 0.05$; Fig.

303 6a). The net changes in the 0-10 cm sediment inorganic P fraction (readily available P_i + Fe/Al-

304 P_i + Ca/Mg-P_i) (range = -8 to +18 g P m^{-2}) and the NaOH-P_o fraction (range = -3 to +8 g P m^{-2})

305 also significantly decreased with distance from the BCS inflow (r^2 = 0.53 and 0.44, respectively,

306 p < 0.01 in both cases; Fig. 6b and 6c). The net change in 0-10 cm sediment residual P typically

307 fell in the range of +6 to +8 g P m^{-2} and was not correlated with distance from the BCS inflow

308 (Fig. 6d).

309   The total P deposition ($P_{deposited}$) in the LPE for the distance in km (x) covered by the

310 sampling (0 to 35 km from BCS inflow, corresponding to area of 974 km^2) was estimated using

311 the following two models (Fig. 7):

312       $$P_{deposited} = -0.4544x + 19.724$$ [2]

313       $$P_{deposited} = -0.0126x^2 + 0.0006x + 11.779$$ [3]

314 Equation 2 represents the regression model shown in Fig. 6a, while Equation 3 corresponds to

315 the lower 95% confidence interval line for that same model in Fig. 6a. When applied in GIS (Fig.

316 6), Equations 2 and 3 resulted in estimates of total P deposition in the LPE during the diversion

317 event equal to 9,614 and 5,114 metric tons P, respectively. As discussed below, the latter, more

318 conservative estimate is likely closer to reality.

319 **4. Discussion**

320 *4.1. Spatial distribution of net change in sediment P*

321   A spatial gradient of change in sediment P content and composition with distance from

322 the BCS inflow was clearly present in the LPE following the 2011 diversion (Figs. 6 and 7). The

323 net increases in sediment total P, inorganic P (readily available P_i + Fe/Al-P_i + Ca/Mg-P_i), and

324 NaOH-P_o were greatest in the region nearer to the BCS inflow (Figs. 5 and 6), which is where

14

325 most inorganic solids settled out of suspension as the river water plume entered and moved

326 eastward through the LPE (Fig. 4). Residual P increased at all sample sites post-diversion, with

327 no spatial pattern (Fig. 6d). We hypothesize that these residual P increases were caused primarily

328 by the settling of finer inorganic solids containing P in stable mineral phases that could stay in

329 suspension and mix throughout the LPE (e.g., clay particles with tightly bound P not extracted

330 with KCl, NaOH, or HCl solutions). The observed decreases in Ca/Mg-P_i in both sediment

331 intervals at "far" sites were likely due to the lower mean Ca contents of the sediments post-

332 diversion (i.e., the sediments were different), rather than movement of P out of the relatively

333 stable Ca/Mg-P_i fraction within the same surface sediment. The differences in Ca content could

334 have been caused by deposition of new sediments, localized sediment heterogeneity at individual

335 sites, or a combination of both. Furthermore, fragments of shell material, common throughout

336 LPE sediments, may have influenced these findings (Flocks et al. 2009). Contents of Al, Fe, and

337 Mg across all sites (and for Ca at "near" sites) were more similar for pre- and post-diversion

338 sediments (Table 1), which increases our confidence that changes in P pools were in general not

339 an artifact of sampling caused by sediment heterogeneity at each site, with the potential

340 exception of Ca/Mg-P_i at "far" sites.

341   Besides the findings noted above, the changes that we observed in P pools after the

342 diversion event were generally not accompanied by changes in non-P-constituents. We believe

343 that this can be explained by the fact that surface sediments in the region of the LPE that we

344 studied have been shaped by their degree of exposure to past BCS events. For example, the

345 surface sediments of the estuary in the region near the BCS are sandier than those in the LPE

346 center (Flocks et al. 2009, Roy and White 2012), and there were already several differences in

15

347   sediment chemistry between "near" and "far" sites pre-diversion (Table 1). However, P can leach

348   out of these sediments over time as the Fe-bound pool is subjected to reduced conditions and the

349   P becomes mobile (Roy et al. 2012). Like P, N can also be lost from the sediments over time due

350   to mineralization and release of NH_4^+ to the water column (Roy and White 2012, Roy et al.

351   2013), which may explain the increase in TN for the "far" sites post-diversion after new

352   sediments were deposited (Table 1). We speculate that ≤ 5 cm of sediment was deposited at

353   some sites monitored (Fabre 2012), therefore our observations of P changes in the 5-10 cm

354   intervals (Fig. 5) were likely caused by mixing of the 0-10 cm sediment layer via wind

355   resuspension, a common phenomenon in the LPE (Flocks et al. 2009).

356   The estimates of total P deposition from the two models we applied (5,114 to 9,614

357   metric tons P) are greater than the BCS discharge of P predicted in USGS reports (Mize et al.

358   2012, Welch et al. 2014). Mize et al. (2012) estimate that between 3,342 and 3,518 metric tons of

359   P was discharged through the BCS into the LPE in 2011. Similar values have been reported by

360   Welch et al. (2014). These two USGS studies calculated P flux using identical surface water

361   measurements collected approximately 2 miles from the diversion gates (less than halfway from

362   gates to the LPE; USGS 300115090245000). However, estimating the total P load into the LPE

363   is challenging given the difficulty of obtaining a sample representative of the entire water

364   column. Samples from middle and lower depths, in addition to surface water, are needed to

365   capture the P associated with the heavier sediment fractions and avoid underestimation of total P

366   flux (Mayer et al. 1998, Sutula et al. 2004). Furthermore, river water flowing through the BCS

367   erodes and transports material from within the spillway into the LPE. We observed large debris

368   flowing through the LPE at stations near the BCS during the peak flow of the 2011 diversion.

369 The influence of spillway erosion, including that occurring after the USGS monitoring site, on

370 the particulate P load into the LPE has not been quantified. It is also worth noting that the

371 discharge of freshwater from LPE northern tributaries was very low during the sampling period

372 due to local drought conditions (Roy et al. 2013), suggesting little, if any, influence of watershed

373 P loading on our findings for sediments within the LPE. Considering prior lower estimates of P

374 diverted through the BCS in 2011, we believe that our more conservative estimate of P

375 deposition in LPE sediments (approximately 5,000 metric tons P based on Equation 3) is likely

376 more accurate than the higher value predicted by Equation 2. For future BCS openings, we

377 recommend water sampling at multiple depths occur across the BCS inlet within the LPE to

378 obtain better estimates of what enters the estuary. Coupling such measurements with sediment P

379 measurements would better constrain estimates of total P input and deposition.

380 *4.2. Stability of P deposited in sediments*

381 We collected the post-diversion sediment cores on July 7th, when water column SRP was

382 still depleted throughout much of the LPE and surface water phytoplankton biomass had

383 declined following a short-lived bloom of non-harmful algae (Fig. 2, Roy et al. 2013 and 2016).

384 Therefore, some of the new P detected in sediments may have been mobilized relatively quickly

385 during the water column SRP rebound period that followed (Fig. 2). However, this was likely a

386 small fraction of the added P. Assuming a water column depth of 3.7 m (LPE average) and a

387 water column equilibrium P concentration of 0.08 mg SRP-P L^{-1} (highest observed concentration

388 at which SRP stabilized in late July 2011 following SRP rebound), we estimate that up to 0.3 g P

389 m^{-2} of sediment P may have been released to the water column during the SRP rebound period.

390   This suggests that most new post-diversion sediment P remained in place during the summer of

391   2011 and beyond, particularly for the region near the BCS inflow.

392   The P fractionation scheme that we employed here is operational and intended to capture

393   a gradient of P stability (Richardson and Reddy 2013). All P pools that we have quantified are

394   dynamic. While readily available P_i, Fe/Al-P_i, and NaOH-P_o are relatively more likely to become

395   soluble and available for flux to the water column, more stable P fractions (e.g., more recalcitrant

396   organic P) can potentially also be solubilized over longer periods (Richardson and Reddy 2013).

397   The Ca/Mg fraction (e.g., apatite minerals) can be formed by precipitation of SRP and Ca/Mg

398   during early diagenesis or formation of diatom-derived polyphosphates, and can be considered

399   stable, only becoming available with a significant drop in pH (Ruttenberg and Berner 1993,

400   Adhikari et al. 2015). The large fractions of TP associated with Ca/Mg-P_i that we report here

401   (Fig. 5), are consistent with the distribution of Ca/Mg-P_i in sediments from the northern Gulf of

402   Mexico's estuaries and shelf (Huanxin et al. 1994, Sutula et al. 2004, Adhikari et al. 2015).

403   Similarly, Ca-bound P has been shown to represent the dominant P fraction for Lake

404   Okeechobee (Moore et al. 1998), Everglades stormwater treatment areas (White et al. 2004), and

405   Florida Bay (Zhang et al. 2004) in Florida, USA. Some sediment P may move into more

406   recalcitrant P forms over the long-term as diagenesis unfolds (e.g., growth of stable apatite

407   minerals at the expense of organic P; Ruttenberg and Berner 1993). Redox reactions influencing

408   the Fe/Al pool, biotic mineralization of organic P (including organic P within the residual

409   fraction), and diagenetic transfer associated with the Ca/Mg pool will largely control sediment P

410   solubility and burial over time (Ruttenberg and Berner 1993, Reddy et al. 1999).

411   Approximately 20-30% of P in LPE sediments existed as readily available P_i, Fe/Al-P_i,

412   and NaOH-P_o post-diversion in 2011 (Fig. 5). This suggests that a substantial amount of

413   sediment P in the LPE can contribute to internal P loading over short to medium time scales. The

414   rate of Fe/Al-P_i release will be greatest under anaerobic conditions due to redox reactions

415   involving Fe (Zhang et al. 2012). The concentration in solution where no net P adsorption or

416   desorption occurs is commonly referred to as the equilibrium SRP concentration (Pant and

417   Reddy 2001). Anaerobic intact sediment core incubations for LPE sediments have indicated a

418   greater water column equilibrium SRP concentration for cores collected near the BCS inflow

419   (0.08 mg P L^{-1}) compared to the central and northwest regions of the estuary (0.06 mg P L^{-1})

420   (Roy et al. 2012). Field measurements have confirmed these concentrations (Roy et al. 2013),

421   suggesting that LPE surface sediments can be anaerobic in the field, despite aerobic overlying

422   waters. Greater equilibrium SRP concentrations near the BCS inflow may be due to historic

423   sediment P loading from diversion events (Fig. 6). Based on our findings in the present study, we

424   expect that the contribution of diversion-related sediment P to internal P loading will persist

425   longest in sediments proximal to the BCS inflow.

426   Estimating the longevity of impact on the estuary for P deposited by diversions in

427   sediments, or "legacy P effect" (Reddy et al. 2011, Jarvie et al. 2013), would require monitoring

428   and dynamic simulation modeling that is beyond the scope of this study. The model would need

429   to include internal P loading rate, water column nutrient levels and food web dynamics, P

430   loading from the watershed, water circulation pattern, particle settling rates, and sediment P

431   biogeochemistry (redox reactions, mineralization of organic P, dynamics of different P pools).

432   For the BCS, repeated openings more closely spaced in time may have a greater effect on

433 internal P loading. The average return time of the BCS opening since construction in 1932 is 6.6

434 years per opening, while the return time of the last two opening since 2008 (2011 and 2016)

435 occurred at 3 and 5 year intervals.

436 *4.3. Implications for Mississippi River diversions*

437   Restoring coastal Louisiana requires successfully navigating a diverse suite of

438 stakeholder interests and desired management goals (State of Louisiana 2017, Peyronnin et al.

439 2017). Large-scale Mississippi River diversions will transport much needed sediment to

440 deteriorating coastal regions (Day et al. 2016), but also nutrients (Roy et al. 2013). Our findings

441 here illustrate directly, for the first time, that Mississippi River diversions can deposit a

442 substantial amount of P in estuarine sediments, much of which is relatively available for release

443 to the overlying water over time. This internal source of P to the water column represents an

444 indirect mechanism that may support summertime blooms of cyanobacteria (especially N-fixers),

445 which can potentially have detrimental effects on coastal fisheries. For example, Garcia et al.

446 (2010) demonstrated the potential for *Microcystis* and *Anabaena* blooms to produce toxins that

447 may accumulate in the tissues of blue crabs and be transferred to higher level consumers,

448 including humans. Ultimately, the urgent need to maintain and build land in coastal Louisiana

449 (Day et al. 2016, Twilley et al. 2016), as well as beneficial impacts of nutrient loading on coastal

450 fisheries (Cowan et al. 2008), may outweigh this eutrophication risk. Nevertheless, we

451 recommend that eutrophication be considered carefully during the planning of restoration

452 activities. Diversion designs that promote greater sedimentation in marsh environments versus

453 shallow bays can likely help limit the eutrophication risk posed by P accumulation in estuarine

454 sediments. Coastal managers should implement a monitoring program for toxin-producing

455 cyanobacteria in the mid to late summertime period in estuarine areas under influence of

456 diversions to provide timely alerts to fisheries groups and the public of potential health concerns.

5. Conclusions

458 Our findings support the following conclusions:

459 1) The 2011 diversion of Mississippi River water through the Bonnet Carré Spillway resulted in

460   substantial net P increase in Lake Pontchartrain Estuary sediments (up to +24 g P m^{-2} for the

461   0-10 cm layer), which decreased with distance from the spillway. We estimate that $\geq 5,000$

462   metric tons of P was deposited in the estuary's sediments during the 2011 diversion.

463 2) Sediment P fractionation results demonstrated increases in inorganic P forms (readily

464   available P_i and Fe/Al-P_i) and more labile organic P (NaOH-P_o) post-diversion in the region

465   near the BCS inflow. The residual P pool accounted for a substantial amount of new

466   sediment P after the diversion regardless of location, likely reflecting the contributions of

467   newly settled fine clay particles with strongly held P_i.

468 3) Readily available Pi, Fe/Al-Pi, and NaOH-Po deposited in LPE sediments (e.g., 45% of total

469   P increase in the 0-5 cm layer for "near" samples, Fig. 5a) likely becomes soluble over time

470   due to redox reactions involving Fe and biotic mineralization of organic P. Over time, this

471   can contribute to internal SRP loading to the water column, which may enhance the potential

472   for eutrophication, including harmful blooms of toxin-producing cyanobacteria (especially

473   nitrogen fixers). More research is needed to quantify how P deposited in estuarine sediments

474   during diversion events can influence the overlying water column, and for how long.

475 4) Eutrophication risk posed by Mississippi River diversions, including symptoms that are

476   indirect due to sediment P impacts, should be considered carefully during the planning of

21

477   restoration efforts in coastal Louisiana. We stress that this is one factor among many to

478   consider during the planning process and development of monitoring activities. Diversion

479   designs that encourage sedimentation in coastal marshes versus open bays can likely reduce

480   the chances that deposited particulate P creates eutrophication risk.

488
References
490

491 Adhikari, P.L., White, J.R., Maiti, K., Nguyen, N., 2015. Phosphorus speciation and sedimentary
492 phosphorus release from the Gulf of Mexico sediments: Implications for hypoxia. Estuarine,
493 Coastal and Shelf Science 164, 77-85.

494 Anderson, J.M., 1976. An ignition method for determination of total phosphorus in lake
495 sediments. Water Research 10, 329-331.

496 Bargu, S., White, J.R., Li, C., Czubakowski, J., Fulweiler, R.W., 2011. Effects of freshwater
497 input on nutrient loading, phytoplankton biomass, and cyanotoxin production in an oligohaline
498 estuarine lake. Hydrobiologia 661, 377-389.

499 Cowan, J.H., Grimes, C.B., Shaw, R.F., 2008. Life history, history, hysteresis, and habitat
500 changes in Louisiana's coastal ecosystem. Bulletin of Marine Science 83, 197-215.

501 Day, J.W., Pont, D., Hensel, P.F., Ibanez, C., 1995. Impacts of sea-level rise on deltas in the Gulf
502 of Mexico and the Mediterranean: the importance of pulsing events to sustainability. Estuaries
503 18, 636-647.

504 Day, J.W., Lane, R.R., D'Elia, C.F., Wiegman, A.R.H., Rutherford, J.S., Shaffer, G.P., Brantley,
505 C.G., Kemp, G.P., 2016. Large infrequently operated river diversions for Mississippi delta
506 restoration. Estuarine, Coastal and Shelf Science 183, 292-303.

507 DeGroot, C.J., Golterman, H.L., 1990. Sequential fractionation of sediment phosphate.
508 Hydrobiologia 192, 143-148.

509 DeLaune, R.D., Gambrell, R.P., Jugsujinda, A., Devai, I., Hou, A., 2008. Total Hg, methyl Hg
510 and other toxic heavy metals in a northern Gulf of Mexico estuary: Lake Pontchartrain basin.
511 Journal of Environmental Science and Health Part A 43, 1006-1015.

512 Fabre, J.B., 2012. Sediment flux and fate for a large-scale diversion: the 2011 Mississippi River
513 flood, the Bonnet Carré Spillway, and the implications for coastal restoration in south Louisiana.
514 M.S. Thesis. Louisiana State University.

515 Flocks, J., Kindinger, J., Marot, M., and Holmes, C., 2009. Sediment characterization and
516 dynamics in Lake Pontchartrain, Louisiana. Journal of Coastal Research 54(SI), 113-126.

517 Garcia, A.C., Bargu, S., Dash, P., Rabalais, N., Sutor, M., Morrison, W., Walker, N.D., 2010.
518 Evaluating the potential risk of microcystins to blue crab (*Callinectes sapidus*) fisheries and
519 human health in a eutrophic estuary. Harmful Algae 9, 134-143.

520 Giosan, L., Syvitski, J., Constantinescu, S., Day, J., 2014. Climate change: protect the world's
521 deltas. Nature 516, 31-33.

522 Golterman, H.L., 1996. Fractionation of sediment phosphate with chelating compounds: a
523 simplification, and comparison with other methods. Hydrobiologia 335, 87-95.

524 Huanxin, W., Presley, B.J., Armstrong, D., 1994. Distribution of sedimentary phosphorus in Gulf
525 of Mexico estuaries. Marine Environmental Research 37, 375-392.

526 Jarvie, H.P., Sharpley, A.N., Spears, B., Buda, A.R., May, L., Kleinman, P.J.A., 2013. Water
527 quality remediation faces unprecedented challenges from "legacy phosphorus". Environmental
528 Science and Technology 47, 8997-8998.

529 Junk, W.J., Bayley, P.B., Sparks, R.E., 1989. The flood pulse concept in river-floodplain
530 systems. p. 11-127 in D.P. Dodge (ed.), Proceedings of the International Large River
531 Symposium. Can. Spec. Publ. Fish. Aquat. Sci. 106.

532 Li, C., Walker, N., Hou, A., Georgiou, I., Roberts, H., Laws, E., McCorquodale, J.A., Weeks, E.,
533 Li, X., Crochet, J., 2008. Circular plumes in Lake Pontchartrain estuary under wind straining.
534 Estuarine, Coastal and Shelf Research 80, 161-172

535 Malecki-Brown, L.M., White, J.R., 2009. Phosphorus sequestration in aluminum amended soils
536 from a municipal wastewater treatment wetland. Soil Science Society of America Journal 73,
537 852-861.

538 Mayer, L.M., Keil, R.G., Macko, S.A., Joye, S.B., Ruttenberg, K.C., Aller, R.C. Importance of
539 suspended particulates in riverine delivery of bioavailable nitrogen to coastal zones. Global
540 Biogeochemical Cycles 12, 573-579.

541 Mize, S., Demcheck, D.K., 2009. Water quality and phytoplankton communities in Lake
542 Pontchartrain during and after the Bonnet Carré Spillway opening, April to October 2008, in
543 Louisiana, USA. Geo-Marine Letters 29, 431-440.

544 Mize, S., Demcheck, D.K., Rivers, B.W., 2012. Water quality and phytoplankton communities
545 before, during, and after the Bonnet Carré Spillway openings in 2008 and 2011, Louisiana.
546 *Mississippi River and Tributaries System – 2011 Post Flood Report*. US Army Corps of
547 Engineers.

548 Moore, P.A., Reddy, K.R., Fisher, M.M., 1998. Phosphorus flux between sediment and overlying
549 water in Lake Okeechobee, Florida: spatial and temporal variations. Journal of Environmental
550 Quality 27, 1428-1439.

551 Nittrouer, J.A., Best, J.L., Brantley, C., Cash, R.W., Czapiga, M., Kumar, P., Parker, G., 2012.
552 Mitigating land loss in coastal Louisiana by controlled diversion of Mississippi River sand.
553 Nature Geoscience 5, 534-537.

554 Pant, H.K., Reddy, K.R., 2001. Phosphorus sorption characteristics of estuarine sediments under
555 different redox conditions. Journal of Environmental Quality 30, 1474-1480.

556 Peyronnin, N.S., Caffey, R.H., Cowan, J.H., Justic, D., Kolker, A.S., Laska, S.B.,
557 McCorquodale, A., Melancon, E., Nyman, J.A., Twilley, R.R., Visser, J.M., White, J.R.,
558 Wilkins, J.G., 2017. Optimizing sediment diversion operations: working group recommendations
559 for integrating complex ecological and social landscape interactions. Water. *In Press*.

560 R Core Team, 2015. R: A language and environment for statistical computing. R Foundation for
561 Statistical Computing, Vienna, Austria. https://www.R-project.org/

562 Reddy, K.R., Wang, Y., DeBusk, W.F., Fisher, M.M., Newman, S., 1998. Forms of soil
563 phosphorus in selected hydrologic units of the Florida Everglades. Soil Science Society of
564 America Journal 62, 1134-1147.

565 Reddy, K.R., Kadlec, R.H., Flaig, E., Gale, P.M., 1999. Phosphorus retention in streams and
566 wetlands: a review. Critical Reviews in Environmental Science and Technology 29, 83-146.

Reddy, K.R., Newman, S., Osborne, T.Z., White, J.R., Fitz, H.C., 2011. Phosphorous cycling in the greater Everglades ecosystem: legacy phosphorous implications for management and restoration. Critical Reviews in Environmental Science and Technology 41, 149-186.

Ren, L, Rabalais, N.N., Turner, R.E., Morrison, W., Mendenhall, W., 2009. Nutrient limitation on phytoplankton growth in the upper Barataria Basin, Louisiana: microcosm bioassays. Estuaries and Coasts 32, 958-974.

Richardson, C.J., Reddy, K.R., 2013. Methods for soil phosphorus characterization and analysis of wetland soils. p. 603-638 in R.D. DeLaune, K.R. Reddy, C.J. Richardson, J.P. Megonigal (eds.), *Methods in Biogeochemistry of Wetlands*. SSSA Book Series 10.

Roy, E.D., Smith, E.A., Bargu, S., White, J.R., 2016. Will Mississippi River diversions designed for coastal restoration cause harmful algal blooms? Ecological Engineering 91, 350-364.

Roy, E.D., White, J.R., Smith, E.A., Bargu, S., Li, C., 2013. Estuarine ecosystem response the three large-scale Mississippi River flood diversion events. Science of the Total Environment 458-460, 374-387.

Roy, E.D., Nguyen, N.T., Bargu, S., White, J.R., 2012. Internal loading of phosphorus from sediments of Lake Pontchartrain (Louisiana, USA) with implications for eutrophication. Hydrobiologia 684, 69-82.

Ruttenberg, K.C., Berner, R.A., 1993. Authigenic apatite formation and burial in sediments from non-upwelling continental margin environments. Geochimica et Cosmochimica Acta 57, 991-1007.

State of Louisiana., 2017. Louisiana's comprehensive master plan for a sustainable coast. Available online: http://coastal.la.gov/a-common-vision/2017-coastal-master-plan/

Sutula, M., Bianchi, T.S., McKee, B.A., 2004. Effect of seasonal sediment storage in the lower Mississippi River on the flux of reactive particulate phosphorus to the Gulf of Mexico. Limnology and Oceanography 49, 2223-2235.

Turner, R.E., Dortch, Q., Justic, D., Swenson, E.M., 2002. Nitrogen loading into an urban estuary: Lake Pontchartrain (Louisiana, U.S.A.). Hydrobiologia 487, 137-152.

Turner, R. E., Dortch, Q., Rabalais, N.N. ,2004. Inorganic nitrogen transformations at high loading rates in an oligohaline estuary. Biogeochemistry 68, 411-422.

596 Twilley, R.R., Bentley, S.J., Chen, Q., Edmonds, D.A., Hagen, S.C., Lam, N.S.N., Willson, C.S.,
597 Xu, K., Braud, D., Peele, R.H., McCall, A. 2016. Co-evolution of wetland landscapes, flooding,
598 and human settlement in the Mississippi River Delta Plain. Sustainability Science 11, 711- 731.

599 USEPA (United States Environmental Protection Agency). 1993. Methods of chemical analysis
600 of water and wastes. Environmental Monitoring Support Laboratory, Cincinnati.

601 Welch, H.L., Coupe, R.H., Aulenbach, B.T., 2014. Concentrations and transport of suspended
602 sediment, nutrients, and pesticides in the Lower Mississippi-Atchafalaya River Subbasin during
603 the 2011 Mississippi River Flood, April through July. Scientific Investigations Report 2014-
604 5100. U.S. Geological Survey, U.S. Department of Interior.

605 White, J.R., Reddy, K.R., Moustafa, M.Z., 2004. Influence of hydrologic regime and vegetation
606 on phosphorus retention in Everglades stormwater treatment area wetlands. Hydrological
607 Processes 18, 343-355.

608 White, J.R., Fulweiler, R.W., Li, C., Bargu, S., Walker, N.D., Twilley, R.R., Green, S.E., 2009.
609 Mississippi River Flood of 2008: Observations of a large freshwater diversion on physical,
610 chemical, and biological characteristics of a shallow estuarine lake. Environmental Science &
611 Technology 43, 5599-5604.

612 Zhang, J.Z., Fischer, C.J., Ortner, P.B., 2004. Potential availability of sedimentary phosphorus to
613 sediment resuspension in Florida Bay. Global Biogeochemical Cycles 18, GB4008.

614 Zhang, W., White, J.R., DeLaune, R.D. 2012. Diverted Mississippi River sediment as a potential
615 phosphorus source affecting coastal Louisiana water quality. Journal of Freshwater Ecology 27,
616 575-586.

617
618
619
620
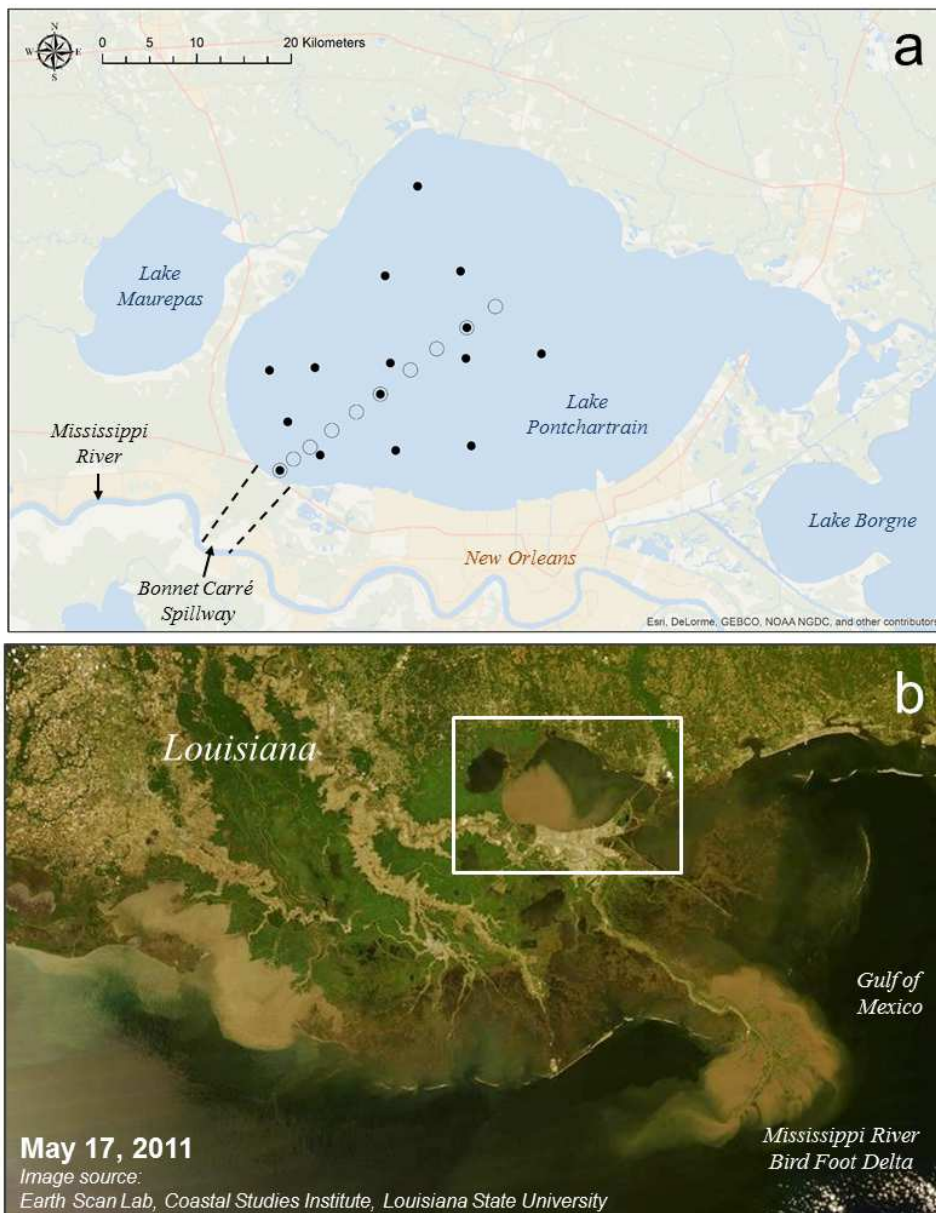
Figure 1. (a) Map of stations sampled in the Lake Pontchartrain Estuary (LPE) during 2011, including 15 locations where sediment cores were collected before and after the Bonnet Carré Spillway (BCS) diversion event (black dots), and a 10-station 30-km transect where water samples were collected for suspended sediment analysis on multiple dates during the event (open circles). (b) MODIS 250 m imagery of coastal Louisiana on May 17, 2011 during the BCS opening provided by the Earth Scan Lab at Louisiana State University. A plume of sediment-rich freshwater can be seen entering the LPE via the BCS and traveling eastward through the estuary (Roy et al. 2016).
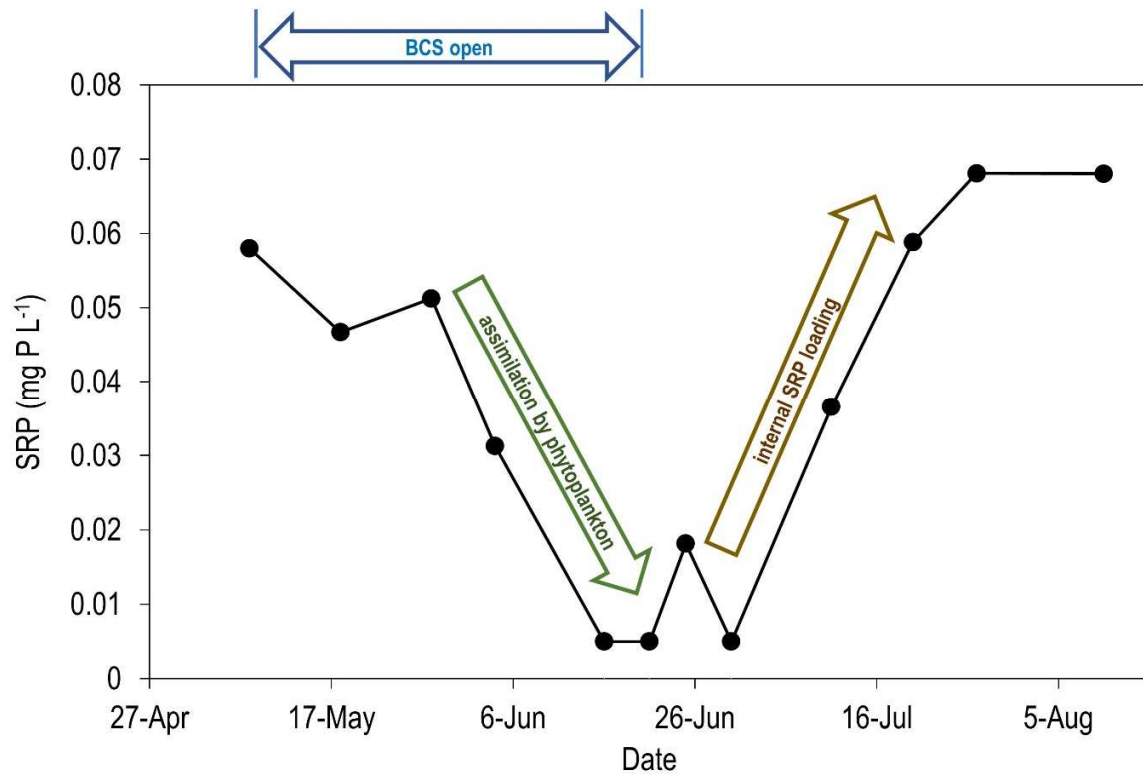
Figure 2. Median surface water (10 cm depth) soluble reactive P (SRP) concentration for the 10-station, 30-km transect in the Lake Pontchartrain Estuary shown in Fig. 1a, illustrating uptake of SRP by phytoplankton, followed by a rebound driven by internal SRP loading. The complete dataset was previously reported in Roy et al. (2013).
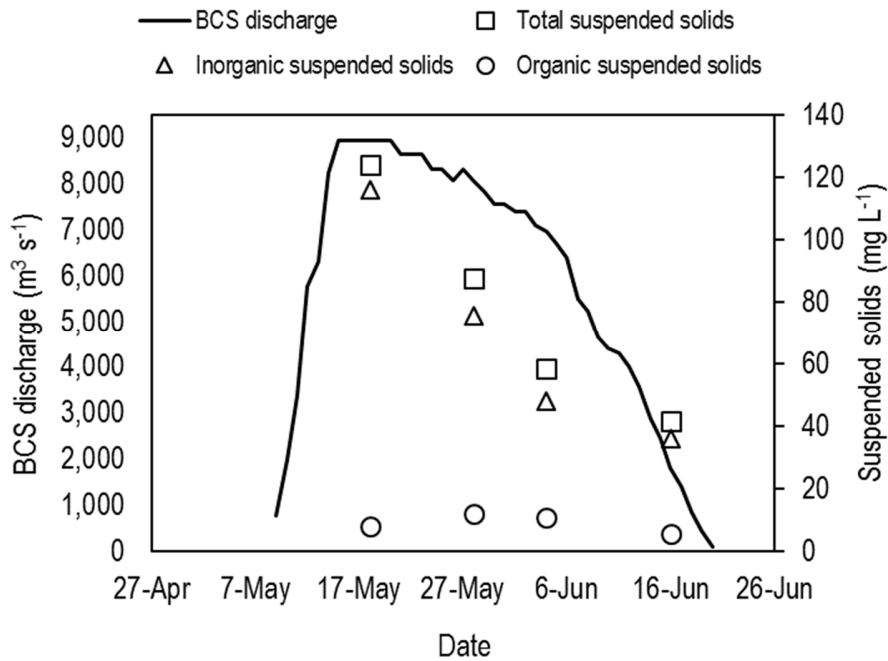
636
637 **Figure 3.** Bonnet Carré Spillway (BCS) discharge (left y-axis) and suspended solids measured
638 0.9 km from the BCS inflow (right y-axis) during the Mississippi River diversion event in 2011.

639
640
641
642
643
644
645
646
647
648
649
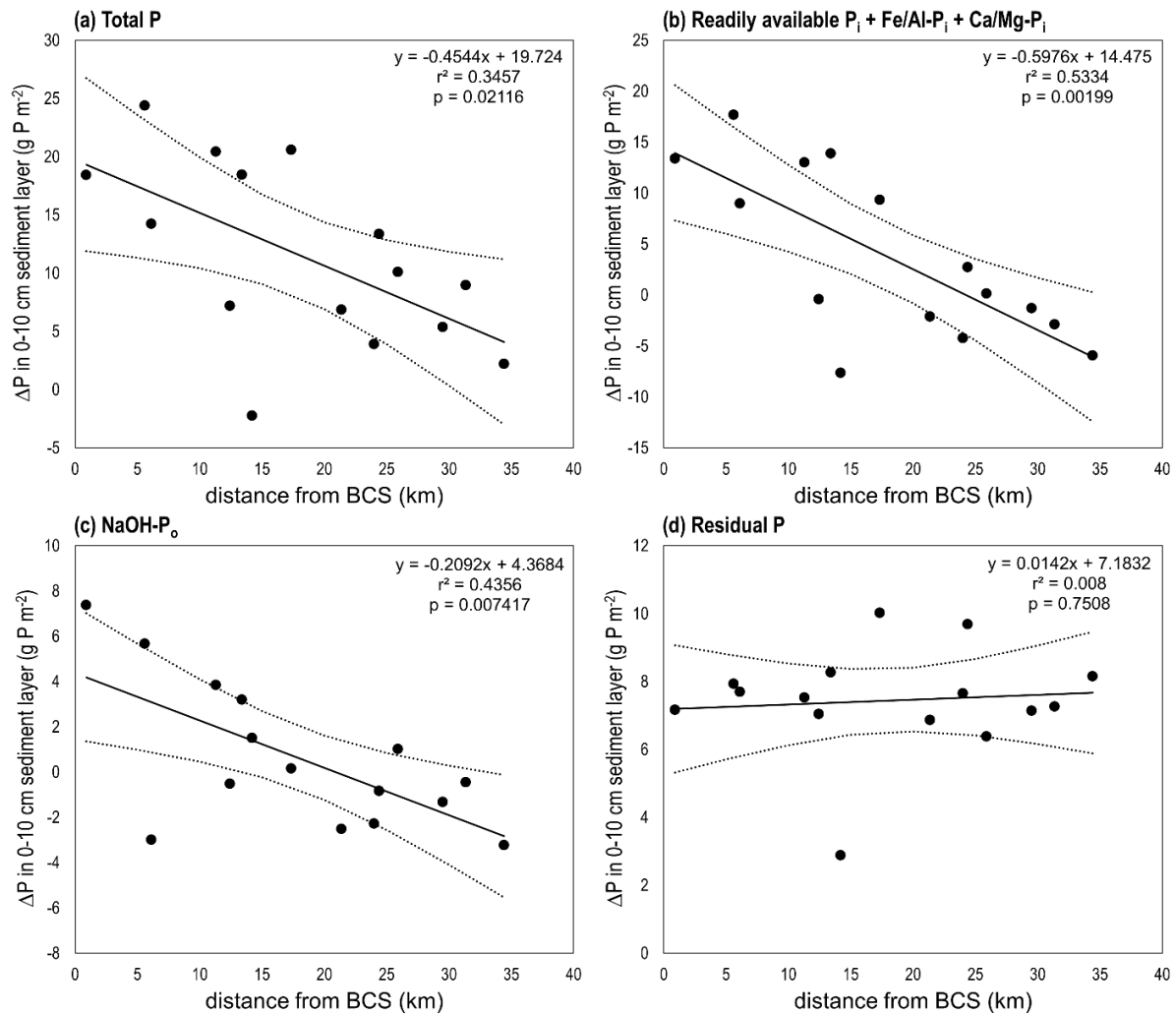650
651
652
653
654
655
656
657
658
659

660
661
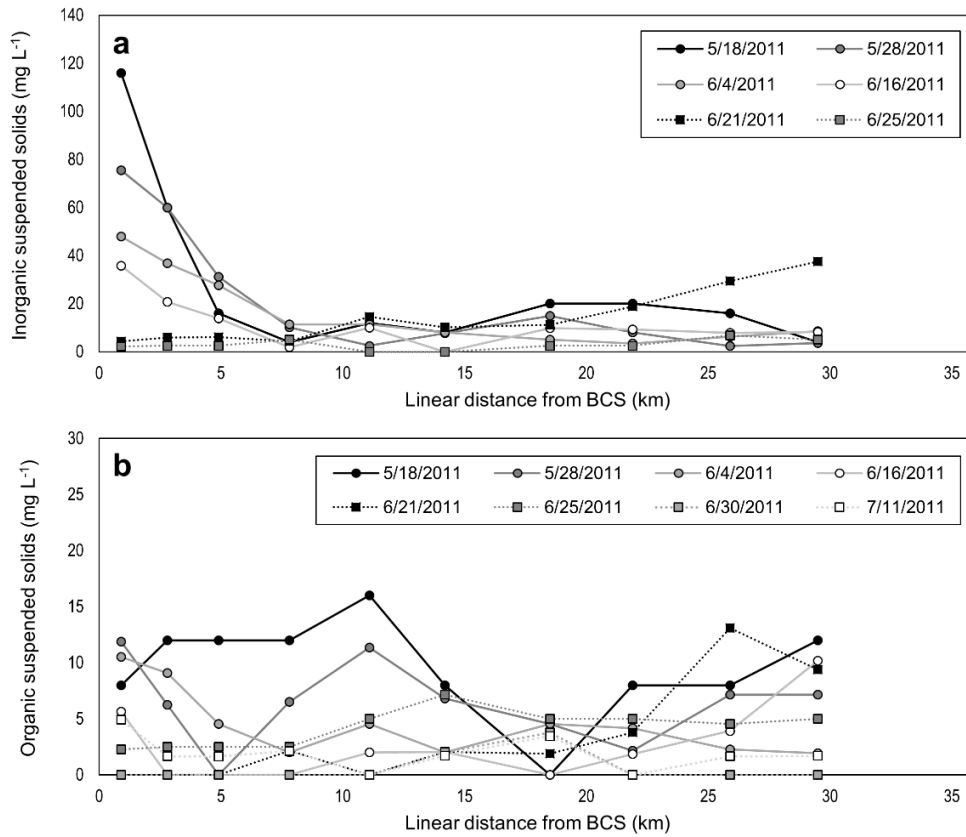
Figure 4. Concentration of (a) inorganic and (b) organic suspended solids in surface waters plotted with linear distance from the BCS inflow. Data are from the 10-station transect in Fig. 1a during (○) and after (□) the BCS diversion event (BCS open from 5/9 to 6/20).

665
666
667
668
669
670
671
672
673
674
675
676
677
678
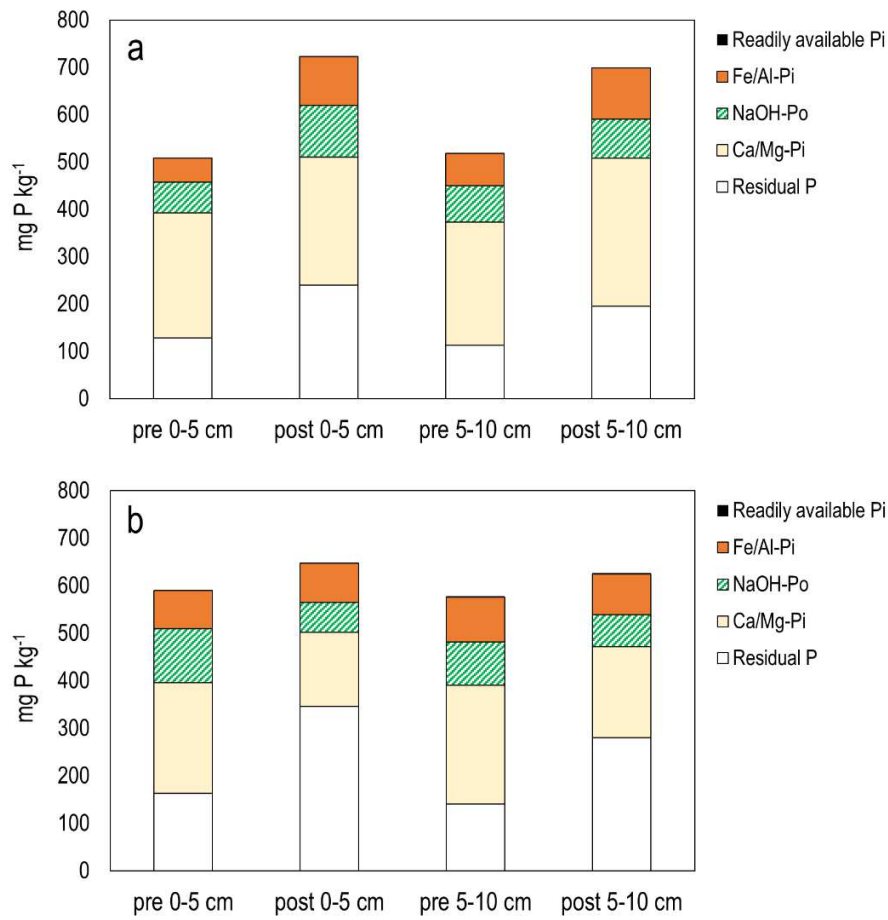
Figure 5. Average phosphorus fractions for sediment samples from (a) "near" ($n = 8$; 1 to 17 km from BCS inflow) and (b) "far" ($n = 7$; 21 to 34 km from BCS inflow) stations collected pre- and post-diversion.
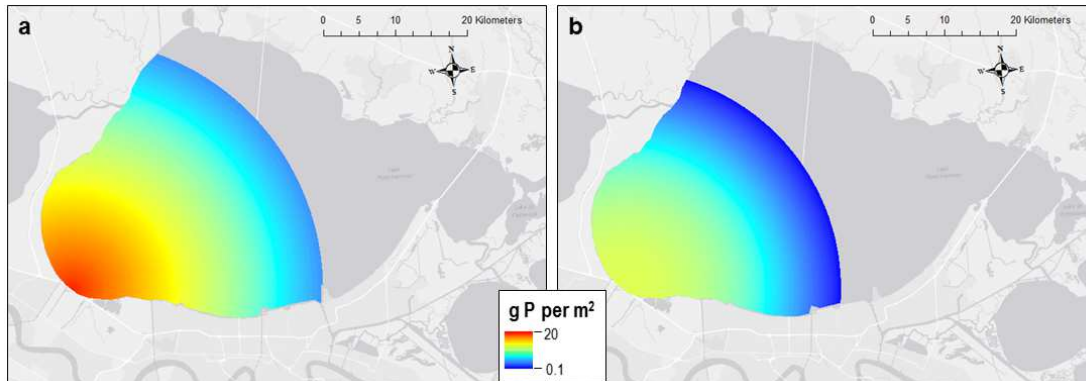
683
684
685
686
687
688
689
690
691
692
693
694
695

(a) Total P

y = -0.4544x + 19.724
r² = 0.3457
p = 0.02116

(b) Readily available P_i + Fe/Al-P_i + Ca/Mg-P_i

y = -0.5976x + 14.475
r² = 0.5334
p = 0.00199

(c) NaOH-P_o

y = -0.2092x + 4.3684
r² = 0.4356
p = 0.007417

(d) Residual P

y = 0.0142x + 7.1832
r² = 0.008
p = 0.7508

Figure 6. Net change in sediment phosphorus (g P m^{-2}) for 0-10 cm sediment layer based on cores collected pre- and post-diversion as a function of distance from the BCS inflow. Positive values indicate an increase in P following the diversion. Linear regression lines (solid) are plotted along with 95% confidence intervals (dotted lines) (n = 15 in all cases). Note that total P in (a) is based on direct total P measurement, not the sum of P fractions. Therefore, the fractions shown in (b), (c), and (d) do not necessarily add up to the value for total P shown in (a) (although the g P m^{-2} values for total P and sum of P fractions are well correlated, r^2 = 0.92).

Figure 7. Spatial distribution of mean net increase in sediment total phosphorus (0-10 cm layer) following the 2011 Bonnet Carré Spillway diversion event as predicted by (a) the regression model in Fig. 6a, and (b) the lower 95% confidence interval for the model in Fig. 6a.

715
716
717
718
719
720
721
722
723
724
725
726
727
728
729
730
731
732
733
734
735
736
737
738

739

Table 1. Physicochemical characteristics of "near" and "far" sediments (mean ± 1 std. deviation) collected in 2011 pre- and post-diversion for 0-5 cm and 5-10 cm sediment intervals ($n = 8$ for each "near" interval-time combination, $n = 7$ for each "far" interval-time combination). Asterisks indicate nonidentical populations for pre-opening versus post-closure comparisons based on Wilcoxon signed-rank tests (* and ** indicate $p \leq 0.05$ and 0.01, respectively). Dagger symbols indicate nonidentical populations for "near" versus "far" comparisons based on Wilcoxon rank-sum tests († and †† indicate $p \leq 0.05$ and 0.01, respectively).

	Near Sediments (1-17 km from BCS inflow)				Far Sediments (21-34 km from BCS inflow)			
	0-5 cm interval		5-10 cm interval		0-5 cm interval		5-10 cm interval	
	pre-opening	post-closure	pre-opening	post-closure	pre-opening	post-closure	pre-opening	post-closure
Total P (mg P kg^{-1})	509 ± 86**	692 ± 43**	500 ± 79**	655 ± 54**	542 ± 21*	660 ± 47*	531 ± 79*	657 ± 33*
Readily available P$_i$ (mg P kg^{-1})	0.5 ± 0.5**	1.1 ± 0.2**	0.9 ± 0.4**	1.8 ± 0.6**	1.1 ± 0.9	1.1 ± 0.1	2.1 ± 1.4	2.2 ± 0.7
Fe/Al-P$_i$ (mg P kg^{-1})	51 ± 35*	103 ± 24*	68 ± 55	108 ± 17†	80 ± 30	82 ± 19	95 ± 94	85 ± 12†
NaOH-P$_o$ (mg P kg^{-1})	65 ± 32†	109 ± 26	77 ± 34	83 ± 32	114 ± 45*†	63 ± 5*	91 ± 33	68 ± 11
Ca/Mg-P$_i$ (mg P kg^{-1})	264 ± 54	271 ± 80†	260 ± 41*	313 ± 54*††	233 ± 39*	156 ± 39*†	250 ± 67*	191 ± 57*††
Residual P (mg P kg^{-1})	128 ± 50**	240 ± 71**††	113 ± 29**	196 ± 40**††	164 ± 29*	346 ± 27*††	140 ± 21*	280 ± 36*††
Moisture content (%)	58 ± 11	62 ± 9††	52 ± 10†	55 ± 9††	70 ± 5*	75 ± 3*††	64 ± 6†	69 ± 4††
Bulk density (g cm^{-3})	0.61 ± 0.21	0.65 ± 0.21†	0.76 ± 0.20††	0.82 ± 0.22††	0.41 ± 0.09	0.40 ± 0.05†	0.44 ± 0.09*††	0.53 ± 0.09*††
Loss on ignition (%)	6.0 ± 2.2†	6.6 ± 1.2††	5.5 ± 1.6††	5.7 ± 1.7†	8.5 ± 1.4†	9.0 ± 1.0††	8.2 ± 1.1††	8.0 ± 1.3†
Total N (%)	0.16 ± 0.04	0.16 ± 0.03††	0.13 ± 0.03	0.13 ± 0.02††	0.20 ± 0.03*	0.23 ± 0.03*††	0.17 ± 0.04	0.20 ± 0.03††
Total C (%)	1.4 ± 0.3	1.5 ± 0.3	1.3 ± 0.2	1.3 ± 0.3†	1.5 ± 0.2	1.7 ± 0.2	1.6 ± 0.4	1.6 ± 0.2†
Al (%)	2.8 ± 1.2†	3.1 ± 0.8††	2.6 ± 0.8††	3.0 ± 0.7††	4.1 ± 0.5†	4.3 ± 0.3††	3.8 ± 0.5††	4.0 ± 0.3††
Fe (%)	2.5 ± 0.7†	2.8 ± 0.5†	2.4 ± 0.5††	2.7 ± 0.4††	3.3 ± 0.3†	3.3 ± 0.1†	3.2 ± 0.3††	3.3 ± 0.2††
Ca (%)	0.9 ± 0.4	0.8 ± 0.3††	0.9 ± 0.4	0.8 ± 0.4	0.7 ± 0.5	0.4 ± 0.1††	1.1 ± 1.0	0.8 ± 0.6
Mg (%)	0.7 ± 0.2†	0.8 ± 0.1†	0.7 ± 0.2	0.8 ± 0.2†	0.9 ± 0.1†	0.9 ± 0.1†	0.9 ± 0.1	1.0 ± 0.1†

745
746

Large-scale Mississippi River diversion into Pontchartrain Estuary

Image source: NASA Earth Observatory

Changes in estuarine sediment phosphorus fractions of varying stability

Legend:
- Readily available Pi
- Fe/Al-Pi
- NaOH-Po
- Ca/Mg-Pi
- Residual P